

Setting a best practice for determining the EGR rate in hydrogen internal combustion engines

S. Verhelst, J. Vancoillie, K. Naganuma, M. De Paepe, J. Dierickx, Y. Huyghebaert

5 *Ghent University, Department of Flow, Heat and Combustion Mechanics,
Sint-Pietersnieuwstraat 41 B-9000 Gent, Belgium*

T. Wallner

Argonne National Laboratory, Argonne, IL, USA

Abstract

10 Exhaust gas recirculation (EGR) is an effective way to reduce NO_x -emissions and increase the efficiency of hydrogen-fuelled internal combustion engines. Knowledge of the exact amount of EGR is crucial to understand the effects of EGR. As the exhaust gas flow is pulsating and chemically aggressive, the flow rate is typically not be measured directly and has to be derived from other
15 quantities. For hydrocarbon fuels, the EGR rate is generally calculated from a molar CO_2 balance, but for hydrogen engines this obviously cannot be used as there are no CO_2 emissions, and consequently no standard practice has been established. This work considers three methods to calculate the amount of EGR in a hydrogen engine. The first one is based upon a volume balance in the mixing
20 section of exhaust gases and fresh air. The second and third method use a molar balance of O_2 and H_2O respectively in this mixing section. The three methods are developed and tested for their accuracy with an error analysis. Additionally, the methods are applied to an experimental dataset gathered on a single cylinder hydrogen engine. Both the theoretical analysis and the exper-
25 imental results confirm the method based on an O_2 molar balance as the most accurate one. The least practical method is the one based on an H_2O balance as it requires additional relative humidity sensors and is less accurate than the others.

Keywords: internal combustion engine, hydrogen, EGR measurement, error
30 analysis

Nomenclature

Symbols

$EGR\%$	mass fraction of EGR [-]
L_s	stoichiometric air-to-fuel ratio [kg/kg]
L_w	actual air-to-fuel ratio [kg/kg]
\dot{m}	mass flow [kg/s]
m_{theor}	theoretical mass capacity of cylinder [kg]
$MW_{a(b)}$	molecular weight of component a (in mixture b) [kg/mol]
n	engine speed [rev/s]
\dot{n}	molar flow rate [mole/s]
p	pressure [Pa]
p_s	saturation pressure (of water) [Pa]
Q	volumetric flow rate [m ³ /s]
R	specific gas constant [J/kg K]
T	temperature [K]
x	MW_{air}/MW_{EGR} [-]
$y_{a(b)}$	mole fraction of component a (in mixture b) [-]

Greek symbols

χ	1/2 for four-stroke engines [-]
δ	absolute error
ΔQ_{air}	as defined in Eq. 4
Δy_{O_2}	as defined in Eq. 13
$\delta y_{H_2O,av}$	average error on the mole fractions of H_2O (see Eq. C.8)
λ	air-to-fuel equivalence ratio [-]
λ_l	volumetric efficiency [-]
ϕ	relative humidity [%]
ρ	density [kg/m ³]

Subscripts

EGR	recirculated exhaust gas
air	air
H_2	hydrogen
mix	intake mixture of fresh air and EGR
O_2	oxygen
$non - O_2$	all gas components except oxygen
dry	all gas components except H_2O

ABDC	after bottom dead centre
ATDC	after top dead centre
BBDC	before bottom dead centre
BTDC	before top dead centre
BMEP	brake mean effective pressure
DC	direct current
ECU	engine control unit
EGR	exhaust gas recirculation
EVC	exhaust valve closing
EVO	exhaust valve opening
H_2 ICE	hydrogen internal combustion engine
ICE	internal combustion engine
IVC	intake valve closing
NO_x	oxides of nitrogen
PFI	port fuel injection
RH	relative humidity
SI	spark ignition
WOT	wide open throttle

1. Introduction

Hydrogen is widely regarded as an attractive alternative for fossil fuels with the possibility of great efficiency and low emissions [1, 2]. The most mature technology using hydrogen as an energy carrier is the internal combustion engine (ICE). To be fully competitive with fossil fuels, a hydrogen fuelled ICE must be able to achieve a comparable performance. However, due to the lower volumetric energy density, a port fuel injection (PFI) hydrogen engine operating stoichiometric at wide open throttle (WOT) has a power deficit of about 15% compared to a gasoline engine [3]. Several strategies have been developed to bridge that power deficit and increase engine efficiency, including supercharging and direct injection, sometimes in combination with exhaust gas recirculation. Direct injection has been shown to increase power and efficiency, while reducing noxious emissions [4]. Supercharging increases the density of fresh air, thus leading to a higher power output. EGR, the subject of this paper, leads to improved efficiency and lower emissions [5, 6].

EGR is a way to allow reliable stoichiometric operation at supercharged conditions, without the occurrence of abnormal combustion phenomena. In [5] this resulted in a maximum power output exceeding that of gasoline operation. Due to the thermal capacity of the EGR gases, the emissions of NO_x , the only hazardous exhaust component of a hydrogen engine, are significantly reduced. Another way to benefit from EGR is by using it to control the engine's power at WOT. This way the pumping losses caused by throttling are avoided, increasing engine efficiency [1].

EGR is a promising engine technology for H_2 ICEs, but unlike most
 60 other engine parameters, the EGR rate is typically not measured directly, but
 rather calculated based on other measured data. For meaningful research on
 the influence of EGR as well as accurate conclusions drawn from such research,
 the correctness of these calculations are vital. However, most H_2 ICE related
 research does not specify the way the amount of EGR is calculated, or does it
 65 vaguely, with no attention to error analysis. This hinders the analysis of results
 and comparison between different studies.

In this paper three methods to calculate the amount of EGR in hydrogen
 fuelled ICEs are developed. For each of these methods a theoretical error anal-
 ysis is performed, and subsequently evaluated by experimental data. Based on
 70 the error analysis a best practice to calculate the EGR% for H_2 ICEs
 is proposed.

2. Methods to determine the EGR rate

2.1. Overview of conceivable methods

The mass fraction of EGR (EGR%) is defined as the mass flow of EGR
 75 divided by the mass flows of EGR, fresh air and fuel:

$$EGR\% = \frac{\dot{m}_{EGR}}{\dot{m}_{EGR} + \dot{m}_{air} + \dot{m}_{H_2}} \quad (1)$$

The mass flows of air and hydrogen can be measured using standard mass
 flow sensors. However, as the pressure of the chemically aggressive exhaust gases
 fluctuates, their mass flow is typically not measured directly. In Figure 1 the
 section where exhaust gases and air are mixed is shown.

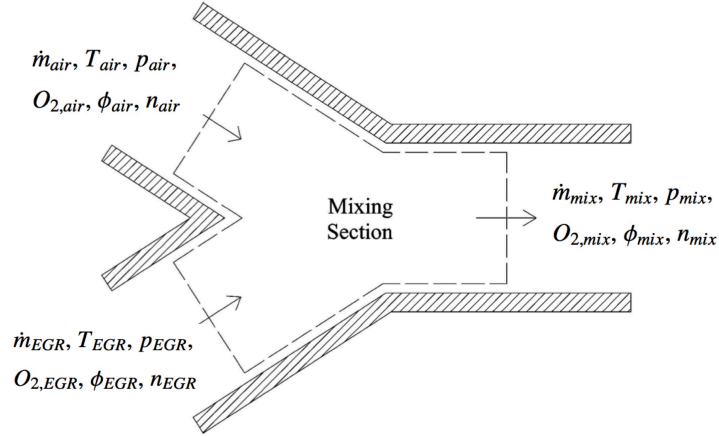
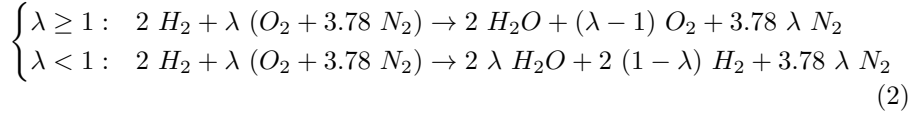


Figure 1: Schematic diagram of the mixing section of exhaust gas and fresh intake
 air

80 The general principle for calculating the EGR rate in hydrocarbon fueled engines is a molar balance of CO_2 , measured in the intake and exhaust. However, as can be seen in the ideal combustion reaction for H_2 with air (2), no CO_2 is generated.



λ is the air-to-fuel equivalence ratio and atmospheric air is assumed to consist of 79.05 vol% N_2 and 20.95 vol% O_2 .

85 Therefore, using a molar balance to determine the EGR rate in hydrogen operation will have to be based on other combustion products like O_2 , H_2O and H_2 . The former two are developed in this work. The H_2 molar balance for EGR determination is not adopted. It requires a non-standard H_2 concentration sensor and for lean mixtures the amount of H_2 in the exhaust gases is low compared to other constituents.

90 Another way to calculate the EGR rate is a volumetric balance in the mixing section. Comparing the intake flow for operation with and without EGR can result in the EGR%, assuming that the volumetric efficiency of the engine remains the same. As this method is relatively easy to implement on a research engine, it will be examined and its principal assumptions will be verified.

95 An energy balance, assuming an adiabatic mixing section, can be applied as well to determine the amount of EGR [7]. However, this method can only be used when the temperature difference between the fresh air and EGR gases is sufficient, because the parameter that determines the EGR rate is the temperature of the mixture. Since the engine in this study uses an EGR cooler (see Section 5), minimizing the temperature difference between air and EGR, this method will not be described in this article.

100 Yet another method is based upon an EGR cooler. When the coolant flow rate, inlet and outlet temperatures, as well as the temperature of the exhaust gases are measured, a heat balance can lead to the EGR rate. However, it is not very practical to measure the coolant flow rate in the EGR cooler. Additionally, the coolant shows no big difference in temperature, which leads to unreliable measurements. For these reasons, this method is not discussed here.

110 2.2. Method 1: Calculation based on constant volumetric efficiency

Assuming that the volume of charge entering the cylinder remains constant irrespective of the mixture's temperature and gas properties, two conditions can be compared: one without and one with EGR. In case of stoichiometric operation this means that the desired load is first set by leaning the mixture, then EGR is gradually added until stoichiometry is reached. The volume of EGR entering the cylinder can then be calculated according to Figure 2. As can be seen, the H_2 volume in the cylinder remains constant in both conditions. It is assumed that an equal H_2 flow with and without EGR results in the same power

output (identical brake thermal efficiency) and gives similar pressure waves in
 120 the intake manifold, resulting in a similar volumetric efficiency [8]. As mentioned
 earlier, however, EGR can slightly increase the brake thermal efficiency. The
 assumption of constant volumetric efficiency for developing Equation 3 is further
 discussed in Section 6.

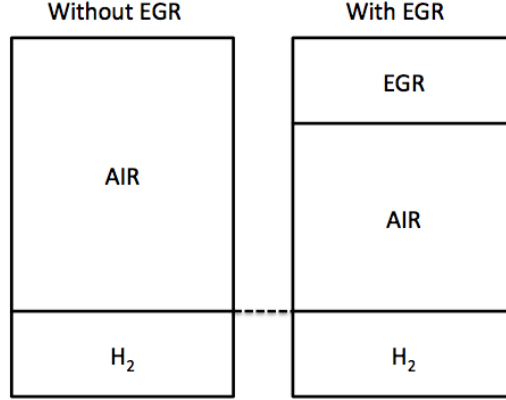


Figure 2: Visualization of the cylinder content with and without use of EGR

This means that the EGR flow rate is equal to the volume of air entering
 125 the cylinder without use of EGR minus the volume of air with use of EGR and
 thus:

$$\dot{m}_{EGR} = \rho_{EGR} \cdot \Delta Q_{air} \quad (3)$$

with:

$$\Delta Q_{air} = Q_{air,0} - Q_{air,1} \quad (4)$$

$Q_{air,0}$ is the volumetric air flow without EGR and $Q_{air,1}$ the volumetric air flow
 with use of EGR. The volumetric air flow can be measured. The density of the
 130 recirculated exhaust gases is calculated through the ideal gas law:

$$\rho_{EGR} = \frac{p_{EGR}}{R_{EGR} \cdot T_{EGR}} \quad (5)$$

with R_{EGR} calculated from the combustion reaction (see Appendix B).

To summarize: this method uses sensors to measure Q_{air} , \dot{m}_{H_2} , p_{EGR} and
 T_{EGR} and has the advantage of its simplicity. A disadvantage is the require-
 ment to measure two operational conditions in order to apply Equation 4: one
 135 without, and one with use of EGR.

2.3. Method 2: Calculation based on the amount of oxygen in the intake and exhaust

Much like the calculation of the EGR rate in conventional hydrocarbon fueled
 ICEs through a CO_2 -balance, an oxygen molar balance can be formulated to

140 determine the EGR rate in an H_2ICE . This molar balance is defined at the mixing section of the exhaust gases and the intake air, before the hydrogen injection (see Figure 1). The theoretical background of this method is described by Szwaja et al. in [9]. Below, a different derivation to find the EGR rate is described.

145 When the EGR mass rate is written as:

$$\dot{m}_{EGR} = \dot{n}_{EGR} \cdot MW_{EGR} \quad (6)$$

With \dot{n}_{EGR} and MW_{EGR} the molar flow rate and molecular weight of the exhaust gases respectively. The molecular weight of the exhaust gases is calculated in Appendix B. To calculate the molar flow rate \dot{n}_{EGR} is written as:

$$\dot{n}_{EGR} = \frac{y_{EGR,mix}}{y_{air,mix}} \cdot \dot{n}_{air} \quad (7)$$

150 With $y_{EGR,mix}$ and $y_{air,mix}$ the mole fractions of EGR and air in the intake mixture. The air mass flow can be measured, which means that through the molecular weight of air (MW_{air}) the air mole rate \dot{n}_{air} is known. The mole fractions $y_{EGR,mix}$ and $y_{air,mix}$ can be calculated as a function of the mole fractions of oxygen in air ($y_{O_2,air}$), EGR ($y_{O_2,EGR}$) and intake mixture ($y_{O_2,mix}$).
155 This relation first has to be derived by substituting the following equations:

$$\begin{cases} MW_{EGR} = y_{O_2,EGR} \cdot MW_{O_2,EGR} + y_{non-O_2,EGR} \cdot MW_{non-O_2,EGR} \\ MW_{air} = y_{O_2,air} \cdot MW_{O_2,air} + y_{non-O_2,air} \cdot MW_{non-O_2,air} \\ MW_{mix} = y_{O_2,mix} \cdot MW_{O_2,mix} + y_{non-O_2,mix} \cdot MW_{non-O_2,mix} \end{cases} \quad (8)$$

into:

$$MW_{mix} = y_{air} \cdot MW_{air} + y_{EGR} \cdot MW_{EGR} \quad (9)$$

Which results in:

$$y_{O_2,mix} = y_{O_2,air} \cdot y_{air,mix} + y_{O_2,EGR} \cdot y_{EGR,mix} \quad (10)$$

Where $non - O_2$ stands for all gas components except oxygen.

160 Substituting $y_{air,mix} = 1 - y_{EGR,mix}$ in Equation 10 and solving for $y_{EGR,mix}$ gives a first expression to substitute in Equation 7. Analogous substitution for $y_{air,mix}$ results in:

$$\dot{n}_{EGR} = \left(\frac{y_{O_2,air} - y_{O_2,mix}}{y_{O_2,mix} - y_{O_2,EGR}} \right) \cdot \dot{n}_{air} \quad (11)$$

Through Equation 6 we obtain the EGR mass rate:

$$\dot{m}_{EGR} = \frac{1}{MW_{air}} \cdot \dot{m}_{air} \cdot MW_{EGR} \cdot \Delta y_{O_2} \quad (12)$$

with:

$$\Delta y_{O_2} = \frac{y_{O_2,air} - y_{O_2,mix}}{y_{O_2,mix} - y_{O_2,EGR}} . \quad (13)$$

The EGR% is now known by substituting Equation 12 into Equation 1.

165 When looking at the derived equation for the EGR% the parameters that have to be measured are \dot{m}_{air} , \dot{m}_{H_2} , $y_{O_2,air}$ in the intake and $y_{O_2,EGR}$ in the exhaust. The first two sensors are normally available on a research engine. They are necessary to determine parameters like λ . Additionally, an O_2 -concentration sensor and the capability to switch between intake and exhaust is
 170 required. Another way to measure the O_2 -content in a gas is with a wide-band lambda sensor. Szwaja et al. used such a sensor in their experiments to measure the oxygen content in the exhaust [9]. This requires a second lambda sensor to measure the O_2 -concentration in the intake mixture. Using a wide-band lambda sensor induces an additional error to the measured oxygen content due to the
 175 conversion of the sensor output voltage to O_2 concentration and the influence of H_2 on the reading [10].

2.4. Method 3: Calculation based on the relative humidity in the intake and exhaust

180 Instead of determining the EGR rate with an oxygen balance, a calculation based on a water balance can be developed as well. The entire derivation of the EGR rate is analogous as in 2.3, however the oxygen concentrations have to be replaced by water concentrations and the subscript 'non - O_2 ' in Equation 8 by 'dry gases', indicating all of the gases except H_2O .

The EGR mass rate is given by:

$$\dot{m}_{EGR} = \frac{1}{MW_{air}} \cdot \dot{m}_{air} \cdot MW_{EGR} \cdot \Delta y_{H_2O} \quad (14)$$

185 with:

$$\Delta y_{H_2O} = \frac{y_{H_2O,air} - y_{H_2O,mix}}{y_{H_2O,mix} - y_{H_2O,EGR}} . \quad (15)$$

Through Equation 1 the EGR% is now known.

The measurement equipment necessary for this method is summarized below included flow sensors to determine \dot{m}_{air} and \dot{m}_{H_2} .

190 Additionally, to determine the mole fractions of water we can rely on the psychometric principles applied on exhaust gases instead of moist air. Consequently, at each of the three sides of the mixing section (Figure 1) a temperature, pressure and relative humidity sensor are necessary to calculate $y_{H_2O,EGR}$; $y_{H_2O,air}$ and $y_{H_2O,mix}$ through:

$$y_{H_2O} = \frac{\phi \cdot p_s}{p} \quad (16)$$

with p_s the saturated water pressure approximated by an equation developed
 195 by Wexler [11]. This equation is a function of temperature and has an accuracy
 of ± 2 Pa. Because of the exponential nature of this function in terms of
 temperature, the position and accuracy of the thermocouples are crucial for
 this method.

However, using a relative humidity sensor in exhaust gases is not obvious be-
 200 cause of calibration issues. The calibration curve of such a sensor is determined
 in a humidity chamber with moist air instead of exhaust gases. Consequently,
 this could give an additional error. Alternatively, a water analyzer could be used
 to determine the water content of the intake mixture. This was not considered
 for in the current work.

205 3. Accuracy of the methods to determine the EGR rate

To find out the best practice to determine the EGR rate, a Taylor accuracy
 analysis was performed on each method of Section 2. Taylor [12] identified the
 error of a random function $q = f(x_1, x_2, \dots, x_n)$ as:

$$\delta q = \sqrt{\left(\frac{\partial q}{\partial x_1} \cdot \delta x_1\right)^2 + \left(\frac{\partial q}{\partial x_2} \cdot \delta x_2\right)^2 + \dots + \left(\frac{\partial q}{\partial x_n} \cdot \delta x_n\right)^2} \quad (17)$$

When applying this equation to the $EGR\%$ functions determined by method 1,
 210 2 and 3 in the previous section, three errors $\delta EGR\%$ are obtained. The method
 that gives the lowest relative error (defined as the ratio $\frac{\delta EGR\%}{EGR\%}$), can be selected
 as the best practice to determine the EGR rate.

3.1. General accuracy equation of the error made on the $EGR\%$

Before studying the accuracy of each method, a general equation describing
 215 the relative error on the $EGR\%$ is developed is used in next subsections. This
 general equation visualizes the parameters having an influence on the dimension
 of the error.

We start from the definition of the $EGR\%$ (Equation 1):

$$EGR\% = \frac{\dot{m}_{EGR}}{\dot{m}_{EGR} + \dot{m}_{air} + \dot{m}_{H_2}} \quad (18)$$

By applying the Taylor method, we obtain the error on the $EGR\%$ (squared):

$$\delta EGR\%^2 = \frac{(\dot{m}_{air} + \dot{m}_{H_2})^2 \cdot \delta \dot{m}_{EGR}^2 + \dot{m}_{EGR}^2 \cdot (\delta \dot{m}_{air}^2 + \delta \dot{m}_{H_2}^2)}{(\dot{m}_{EGR} + \dot{m}_{air} + \dot{m}_{H_2})^4} \quad (19)$$

Equation 19 shows that the error on the $EGR\%$ depends on three errors:
 $\delta \dot{m}_{EGR}$, $\delta \dot{m}_{air}$ and $\delta \dot{m}_{H_2}$. The parameters \dot{m}_{EGR} , \dot{m}_{air} and \dot{m}_{H_2} determine
 the weight of these errors. As explained in Appendix A.1, this equation can be
 reshaped into a general equation for the relative error on the $EGR\%$ (Eq. 20) by

neglecting $\delta\dot{m}_{H_2}$ with regard to $\delta\dot{m}_{air}$, \dot{m}_{H_2} with regard to \dot{m}_{air} and applying the definition of volumetric efficiency λ_l :

$$\left(\frac{\delta EGR\%}{EGR\%}\right)^2 = \frac{1}{(\lambda_l \cdot m_{theor} \cdot n \cdot \chi)^2} \cdot \left(\frac{(1 - EGR\%)^2}{EGR\%^2} \cdot \delta\dot{m}_{EGR}^2 + \delta\dot{m}_{air}^2 \right) \quad (20)$$

220 Where $\chi = \frac{1}{2}$ for four-stroke engines and m_{theor} is the theoretical mass capacity of the cylinder as defined in Appendix A.1. m_{theor} depends on the actual air-fuel ratio (λ), the amount of EGR and the cylinder volume. Assuming that \dot{m}_{EGR} and \dot{m}_{air} are measured with a measuring device with errors $\delta\dot{m}_{EGR}$ and $\delta\dot{m}_{air}$, Equation 20 indicates that the relative error on the EGR% approaches 225 infinity when the EGR% approaches zero. The relative error reaches a minimum when the EGR% is equal to 1, which means that the relative error is a strictly descending function of the EGR%, and thus the more EGR is used, the better the accuracy of the calculated EGR%. Furthermore we see in Equation 20 that at constant EGR% and increasing engine speed or volumetric efficiency (λ_l), 230 the relative error on the EGR% decreases.

As described in Section 1 the EGR mass rate, \dot{m}_{EGR} , is typically not measured directly. As a result, the error $\delta\dot{m}_{EGR}$ depends on the accuracy of the devices used to measure the necessary quantities to apply one of the methods described in Section 2. Therefore, an expression for $\delta\dot{m}_{EGR}$ to substitute in 235 Equation 20 will be developed for each method in the following subsections.

3.2. Accuracy equation of the error on the EGR% for method 1

In Section 2.2 we found that the EGR mass rate is equal to:

$$\dot{m}_{EGR} = \rho_{EGR} \cdot \Delta Q_{air} \quad (21)$$

Applying the Taylor method on this equation, the following equation is obtained after simplification (see Appendix A.2).

$$\left(\frac{\delta EGR\%}{EGR\%}\right)^2 = \frac{1}{(\lambda_l \cdot m_{theor} \cdot n \cdot \chi)^2} \cdot (c_1 \cdot \delta\dot{m}_{air}^2 + c_2 \cdot \delta\dot{m}_{H_2}^2) \quad (22)$$

240 With:

$$\begin{aligned} c_1 &= 2 \cdot \left(\frac{\rho_{EGR}}{\rho_{air}}\right)^2 \cdot \frac{(1 - EGR\%)^2}{EGR\%^2} + 1 + \frac{2698.77}{\left(1 + \frac{0.029}{\lambda}\right)^4} \cdot \frac{1}{R_{EGR}^2} \cdot \frac{1}{\lambda^2} \\ c_2 &= \frac{2698.77 \cdot L_s^2}{\left(1 + \frac{0.029}{\lambda}\right)^4} \cdot \frac{1}{R_{EGR}^2} \end{aligned} \quad (23)$$

Equation 23 shows us that only c_1 approaches infinity when the EGR% approaches zero.

3.3. Accuracy equation of the error on the EGR% for method 2

In Section 2.3 we determined the EGR mass rate as:

$$\dot{m}_{EGR} = \frac{1}{MW_{air}} \cdot \dot{m}_{air} \cdot MW_{EGR} \cdot \Delta y_{O_2} \quad (24)$$

245 As shown in Appendix A.3 applying the Taylor formula gives:

$$\left(\frac{\delta EGR\%}{EGR\%} \right)^2 = \frac{1}{(\lambda_l \cdot m_{theor} \cdot n \cdot \chi)^2 \cdot (c_1 \cdot \delta \dot{m}_{air}^2 + c_2 \cdot \delta \dot{m}_{H_2}^2 + c_3 \cdot \delta y_{O_2}^2)} \quad (25)$$

with:

$$\begin{aligned} c_1 &= \frac{2.7 \cdot 10^{-5}}{\left(1 + \frac{0.21}{\lambda}\right)^4} \cdot \frac{1}{MW_{EGR}^2} \cdot \frac{1}{\lambda^2} + 2 \\ c_2 &= \frac{2.7 \cdot 10^{-5}}{\left(1 + \frac{0.21}{\lambda}\right)^4} \cdot \frac{L_s^2}{MW_{EGR}^2} \\ c_3 &= \frac{\dot{m}_{air}^2}{(y_{O_2,mix} - y_{O_2,EGR})^2} \cdot \left(2 + \frac{2}{x} \cdot \frac{(1 - EGR\%)}{EGR\%} + \frac{1}{x^2} \cdot \frac{(1 - EGR\%)^2}{EGR\%^2} \right) \end{aligned} \quad (26)$$

and $x = \frac{MW_{air}}{MW_{EGR}}$. We see from Equation 25 and 26 that the coefficients c_1 and c_2 are only a function of λ (MW_{EGR} is also a function of λ as can be seen in Appendix B). Coefficient c_3 depends on the air mass flow, the oxygen content in the mixture and exhaust gases, and the EGR%. Decreasing the EGR% increases c_3 .
250

3.4. Accuracy equation of the error on the EGR% for method 3

In Section 2.4 we determined the EGR mass rate as:

$$\dot{m}_{EGR} = \frac{1}{MW_{air}} \cdot \dot{m}_{air} \cdot MW_{EGR} \cdot \Delta y_{H_2O} \quad (27)$$

which is similar to \dot{m}_{EGR} of method 2. Consequently, applying Taylor results in a similar equation as in Section 3.3:
255

$$\left(\frac{\delta EGR\%}{EGR\%} \right)^2 = \frac{1}{(\lambda_l \cdot m_{theor} \cdot n \cdot \chi)^2 \cdot (c_1 \cdot \delta \dot{m}_{air}^2 + c_2 \cdot \delta \dot{m}_{H_2}^2 + c_3 \cdot \delta y_{H_2O,av}^2)} \quad (28)$$

with:

$$\begin{aligned}
c_1 &= 2 + \frac{2.7 \cdot 10^{-5}}{\left(1 + \frac{0.21}{\lambda}\right)^4} \cdot \frac{1}{\lambda^2} \cdot \frac{1}{MW_{EGR}^2} \\
c_2 &= \frac{2.7 \cdot 10^{-5}}{\left(1 + \frac{0.21}{\lambda}\right)^4} \cdot \frac{L_s^2}{MW_{EGR}^2} \\
c_3 &= \frac{\dot{m}_{air}^2}{(y_{H_2O,mix} - y_{H_2O,EGR})^2} \cdot \left(2 + \frac{2}{x} \cdot \frac{(1 - EGR\%)}{EGR\%} + \frac{2}{x^2} \cdot \frac{(1 - EGR\%)^2}{EGR\%^2} \right) \quad (29)
\end{aligned}$$

and $x = \frac{MW_{air}}{MW_{EGR}}$. We see that the only difference between Equation 28 and 25 is the error $\delta y_{H_2O,av}$ and the coefficient c_3 .

4. Experimental Setup

260 4.1. Experimental Equipment

To evaluate the EGR-calculation methods two series of measurements were gathered on a single cylinder two valve 400cc engine modified to operate on hydrogen fuel. The characteristics of the engine are summarized in Table 1 and the engine's layout is shown in Figure 3. The engine is coupled to a DC
265 motor that can work as generator or motor. A MoTeC M4 Pro ECU is used to control the two Teleflex GFI gas injectors and the ignition timing. The setup is equipped with an exhaust gas recirculation line in which an EGR cooler reduces the temperature of the exhaust gases to 25°C. The amount of EGR is controlled by varying the duty cycle of a pulse width modulated EGR valve. The mixture
270 of air and exhaust gases is then led to a compressor where the engine intake pressure can be charged up to 2 bar gauge. The intake charge is cooled in an intercooler and sent through a buffer vessel in the combustion chamber. The buffer vessel dampens the air flow in the duct before the vessel to ensure accurate air mass flow measurements.

275 A first series of measurements focused on the first two methods. The third method was not applied since no humidity sensors were available at the time. Method 2 and 3 were separately analysed in a second set of experiments. Each method requires several sensors, which have their influence on the accuracy of the EGR calculation. In Table 2 the sensors that are used for the experimental validation of the methods are listed with their respective accuracies. For
280 method 2, the O_2 concentration can be measured using a wide band λ sensor (method 2(a)) or an exhaust gas analyser (method 2(b)). For method 3, the humidity of the intake air is assumed to be the same as the atmospheric humidity. A stationary sensor is installed in the lab to measure atmospheric conditions including the humidity. The relative humidity of EGR gas is assumed to be
285 100% as water vapor condensed in the EGR cooler. For the mixed intake gas,

Cylinders	1
Valves	2
Bore/stroke (mm)	77.5/86.4
Displacement (cc)	407.3
Compression ratio	10.17:1
IVO	7°CA BTDC
IVC	66°CA ABDC
EVO	64°CA BBDC
EVC	21°CA ATDC
Injection	PFI

Table 1: Engine characteristics

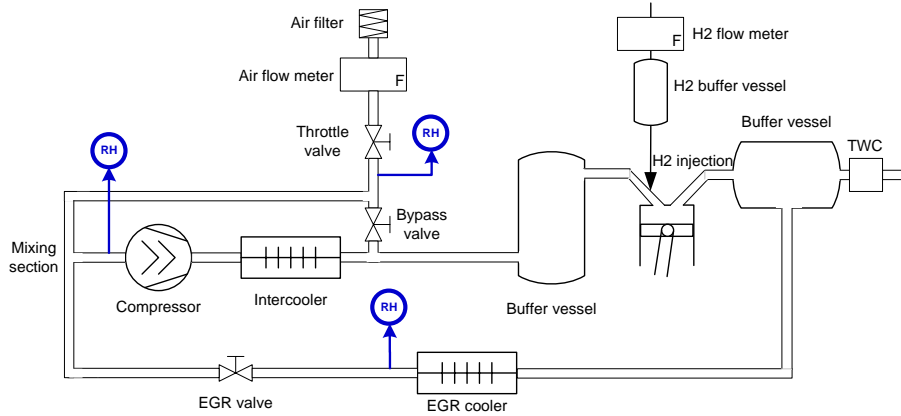


Figure 3: Test engine layout with indicated measuring places for relative humidity (RH)

the relative humidity is measured using a capacitive humidity sensor (Honeywell HIH-4000).

4.2. Experimental Procedure

290 The first set of experiments was taken at different conditions for load, engine speed and EGR rate. The engine speed was varied between 1800 and 3000 rpm, no supercharging was applied and λ was set close to 1 to ensure high conversion efficiencies of the three-way catalyst. Recorded quantities included torque, engine speed, air and hydrogen mass flow, oxygen concentration in intake and exhaust, intake and exhaust pressure and pollutant emissions. The dataset covers a wide range of EGR% in order to investigate the applicability of the methods for low and high EGR rates.

295 The second set of experiments was also obtained in normally aspirated conditions, but λ was not kept constant. Engine speed was varied between 1500 and 2000 rpm and three different H_2 flow rates were considered (2.8, 3.2 and 3.7
300

Device	Variable	Accuracy
Bronkhorst Hi-tec F-106BZ-HD-01-V	air flow	$\delta_{Q_{air}} = 0.6 \text{ m}^3/\text{h}$
Bronkhorst Hi-tec F-113AC-HDD-55V	H_2 flow	$\delta_{Q_{H_2}} = 0.18 \text{ m}^3/\text{h}$
Sick Maihak	O_2 -concentration	$\delta_{O_2} = 0.25 \text{ vol}\%$
Honeywell HIH-4000	relative humidity	$\delta\phi = 3.5\%$
ATAL TRP232-102D	atmospheric rel. hum.	$\delta\phi = 2.5\%$

Table 2: Measuring equipment for EGR analysis

Nm³/hr). Torque was not controlled and depended on the EGR rate, which was varied between lower and upper bounds restricted by back-fire and combustion stability respectively. The EGR and mixture temperatures were not controlled, but depended on the operating conditions, since the coolant flow rate through the EGR cooler was kept constant. This resulted in a wide range of conditions to compare the different methods. The experimental conditions for both datasets are summarized in Appendix E.

5. Results and Discussion

5.1. Theoretical discussion of the accuracy equations

To compare the accuracy of all three methods, variables such as λ and the oxygen content in the mixture ($O_{2,mix}$) have to be substituted in the coefficients c_1 , c_2 and c_3 . In this section, we will simulate realistic values for these variables in order to evaluate these coefficients. Variables that are common for each method are the air-fuel ratio (λ), the amount of EGR (EGR%), the engine speed, the volumetric efficiency and the theoretical mass entering the cylinder (m_{theor}).

λ is set to 1 for the simplicity of substituting this value in the coefficients c_1 , c_2 and c_3 . This value does not differ significantly with λ in the first set of experiments. Choosing stoichiometric conditions implies that:

$$\begin{aligned}
 MW_{EGR} &= 0.0245 \frac{kg}{mol} \\
 R_{EGR} &= 338.8 \frac{J}{kg K}
 \end{aligned} \tag{30}$$

Where both MW_{EGR} and R_{EGR} are calculated as detailed in Appendix B. The relative error increases with decreasing EGR% and engine speed, as described in the previous section. This means that when we want to compare the relative errors of all methods, one of those variables has to remain constant while the other varies. We keep the engine speed constant at 2500 rpm and vary the amount of EGR from 10% to 50%. Because m_{theor} depends on λ and the amount of EGR, this variable is now known at every EGR%. The volumetric efficiency λ_l is estimated to be 85% irrespective of the EGR%.

The errors of the measurement devices are another important set of variables. To allow a comparison between the results of this subsection with the experimental results, we use the same errors as in Section 5.2, except for $y_{H_2O,av}$:

$$\begin{aligned}
\delta\dot{m}_{air} &= 0.775 \frac{kg}{h} \\
\delta\dot{m}_{H_2} &= 0.0162 \frac{kg}{h} \\
\delta y_{O_2} &= 0.25 \% \\
\delta y_{H_2O,av} &= 0.005 \%
\end{aligned} \tag{31}$$

The variables that are inherent to the method are determined as follows:

- Method 1: the coefficients c_1 and c_2 (equation 23) depend on the amount of EGR, λ , R_{EGR} , ρ_{air} and ρ_{EGR} . The values of the first three variables are set as described above. The last two are determined by the ideal gas law and consequently, they depend on the pressure and temperature. If we assume that $T_{EGR} = T_{air}$ and $p_{EGR} = p_{air}$, the ratio $\frac{\rho_{EGR}}{\rho_{air}}$ (to be substituted in c_1) is equal to:

$$\frac{\rho_{EGR}}{\rho_{air}} = \frac{R_{air}}{R_{EGR}} = \frac{286.9 \frac{J}{kg \cdot K}}{338.8 \frac{J}{kg \cdot K}} = 0.85 \tag{32}$$

- Method 2: besides the common variables described above, the coefficients c_1 , c_2 and c_3 depend on \dot{m}_{air} , $y_{O_2,mix}$ and $y_{O_2,EGR}$. The mass air flow is determined as the product of the volumetric efficiency with the theoretical mass air flow. According to the combustion reaction (Equation 2) there is no oxygen in the exhaust gases when working stoichiometrically, which means $y_{O_2,EGR} = 0\%$. The oxygen content in the mixture is calculated as a function of the amount of EGR. Reasoning that $y_{O_2,mix}$ should be equal to $y_{O_2,air}$ ($= 20.95\%$) when the $EGR\% = 0\%$ and equal to $y_{O_2,EGR}$ ($= 0\%$) when the $EGR\% = 100\%$, and assuming a linear function between both values, we get:

$$y_{O_2,mix} = (y_{O_2,EGR} - y_{O_2,air}) \cdot EGR\% + y_{O_2,air} \tag{33}$$

- Method 3: the only difference in variables between method 2 and method 3 is that instead of the oxygen content in the mixture and exhaust gases, the water content ($y_{H_2O,mix}$ and $y_{H_2O,EGR}$) has to be determined. To determine $y_{H_2O,EGR}$ (Equation A.13), we assume $p_{EGR} = 90000 Pa$ and that p_s is calculated (through Wexler's equation) with $T_{EGR} = 25^\circ C$. Because of the great amount of H_2O in the exhaust gases it is very likely that condensation occurs. Therefore, we assume $\phi = 100\%$ which means $y_{H_2O,EGR} = 3.52\%$. The amount of water vapor in the mixture, $y_{H_2O,mix}$,

is determined at $p_{mix} = 90000Pa$, $T_{mix} = 24^\circ C$ and with ϕ_{mix} -similar to $y_{O_2,mix}$ - determined as a function of the amount of EGR:

$$\phi_{mix} = (\phi_{EGR} - \phi_{air}) \cdot EGR\% + \phi_{air} \quad (34)$$

With this simulated dataset, we obtain that the relative error on the EGR% for all three methods varies as a function of the EGR% according to Figure 4. This
 360 Figure is analyzed and discussed in Section 6.

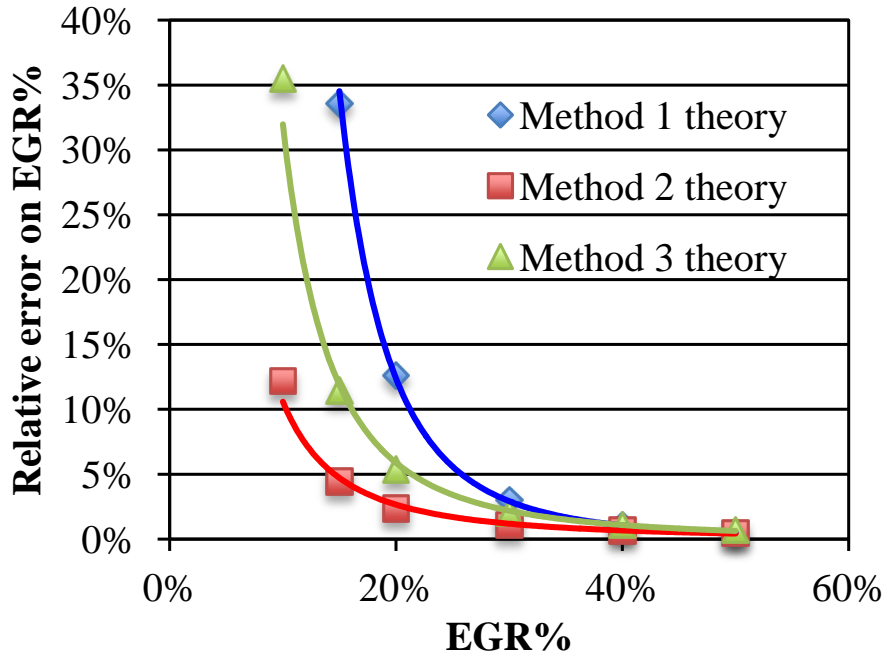


Figure 4: Relative error on the EGR% vs EGR%. Markers: calculation results. Lines: best fits

5.2. Experimental discussion of the accuracy equations

5.2.1. Calculated EGR% for the different methods

In Figure 5 the calculated EGR ratios are compared for method 1 and 2, and for method 2 and 3 using the first and second experimental dataset respectively.
 365 For the second dataset the O_2 concentration was separately measured using both a λ sensor and an exhaust gas analyzer.

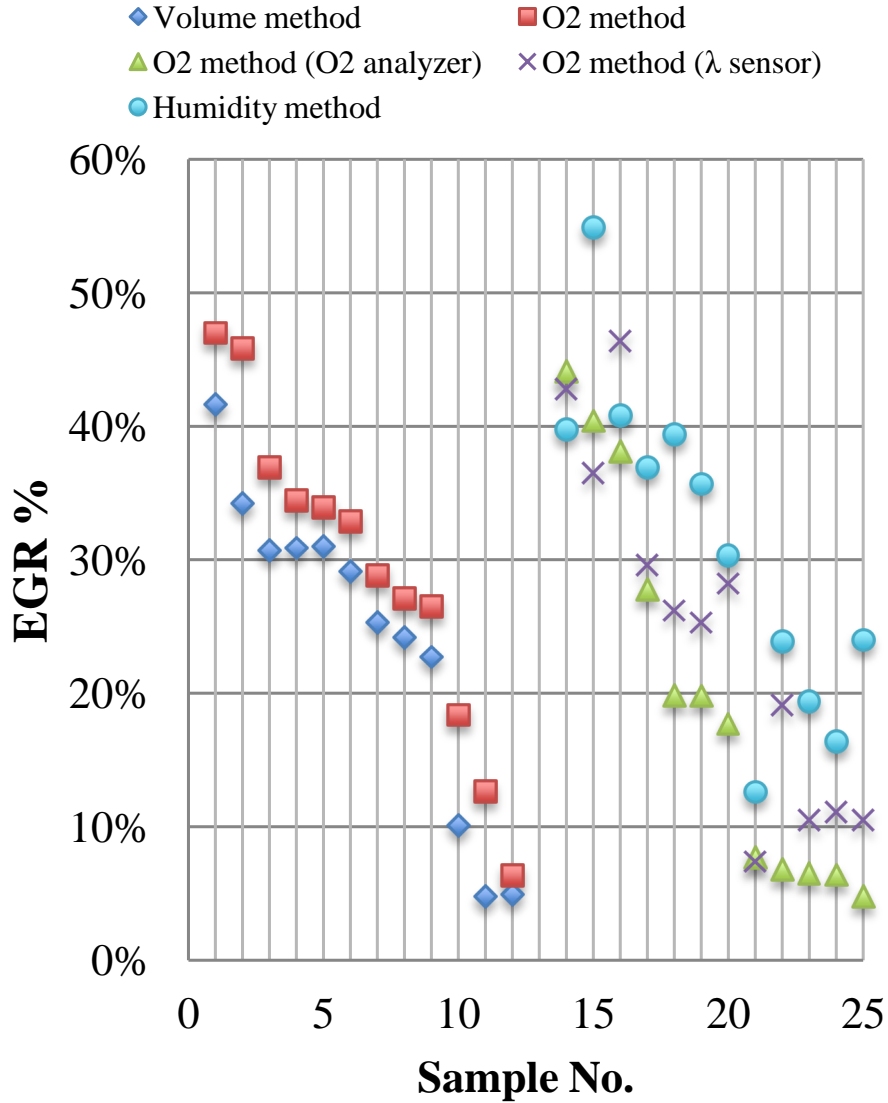


Figure 5: Comparison of the calculated EGR% using different methods. Experimental dataset 1: sample 1-12. Experimental dataset 2: sample 14-25

The EGR% for the first and second method is calculated and visualized for the twelve samples of the first dataset in Figure 5. Both methods follow the same trend, but the second method gives a slightly higher value than the first. This difference originates from the equation of the EGR mass rate as calculated in Section 2. In Appendix D the ratio of equation 3 and 12 is calculated and

370

it is concluded that the offset between both methods depends on the operating parameters of the considered measurement condition.

375 The results for the second dataset show that method 2(a) and 2(b) produce a similar trend, but compared to method 2(a), method 2(b) gives EGR% that are slightly higher for low EGR ratios and slightly lower for high EGR ratios. This is possibly due to the calibration of the λ sensor, which is insufficiently adapted to the very lean mixtures employed in hydrogen operation [10]. Method 3 results in higher values for EGR% at almost all measurement conditions.

380 5.2.2. *The relative error on the EGR%*

In Figures 6 and 7 the relative error on the EGR% calculated using the following methods is compared:

- Volume method (Method 1), with experimental dataset 1
- O_2 method (Method 2), with experimental dataset 1
- 385 • O_2 method using O_2 analyzer (Method 2(a)), with experimental dataset 2
- O_2 method using λ sensor (Method 2(b)), with experimental dataset 2
- Method 3, with experimental dataset 2

390 For method 3, a case study is performed in which the absolute error of the relative humidity sensors was varied between 1.5% and 3.5%. The upper bound represents the accuracy as reported by the manufacturer. The lower bound is the minimum achievable error after additional calibration in a climate room with a known humidity.

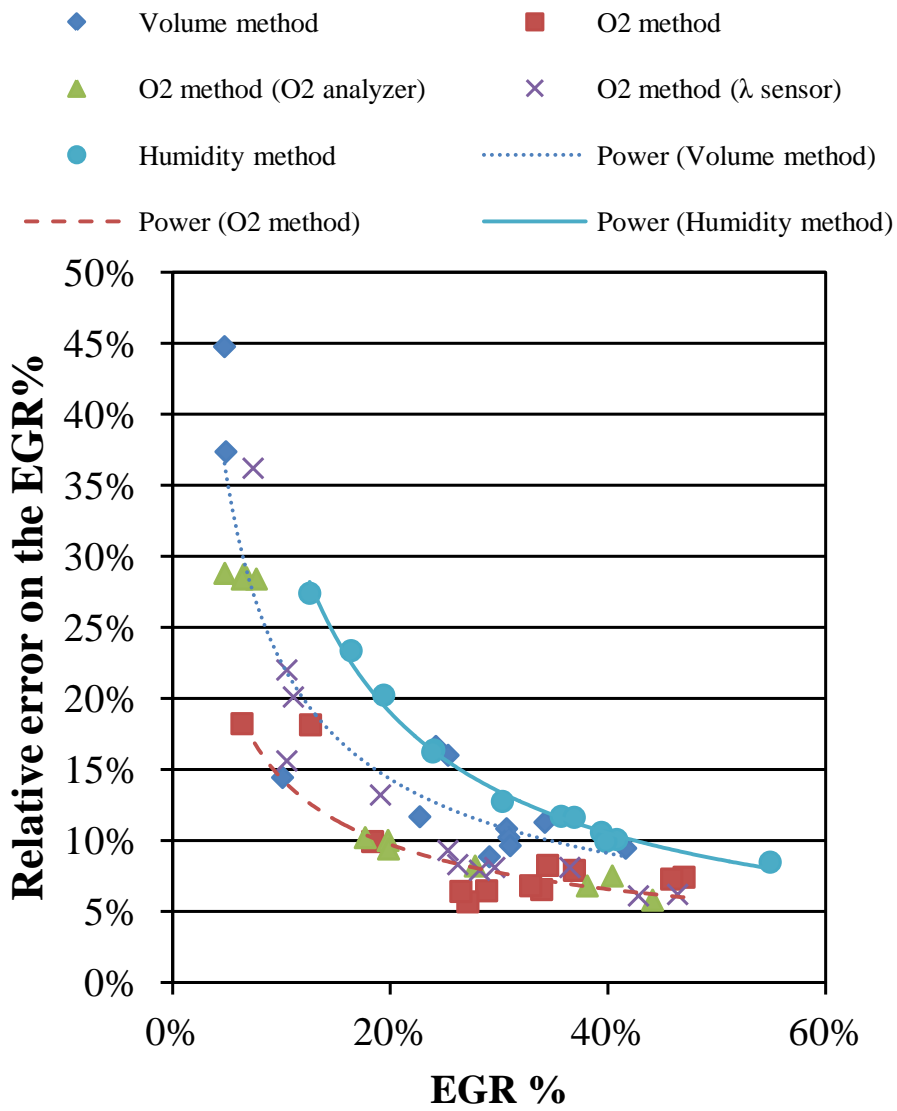


Figure 6: Comparison of the relative error on EGR% calculated using three different methods. Method 1 and 2 - dataset 1. Method 2(a), 2(b) and 3 - dataset 2. Error on the relative humidity $\delta\phi = 1.5\%$

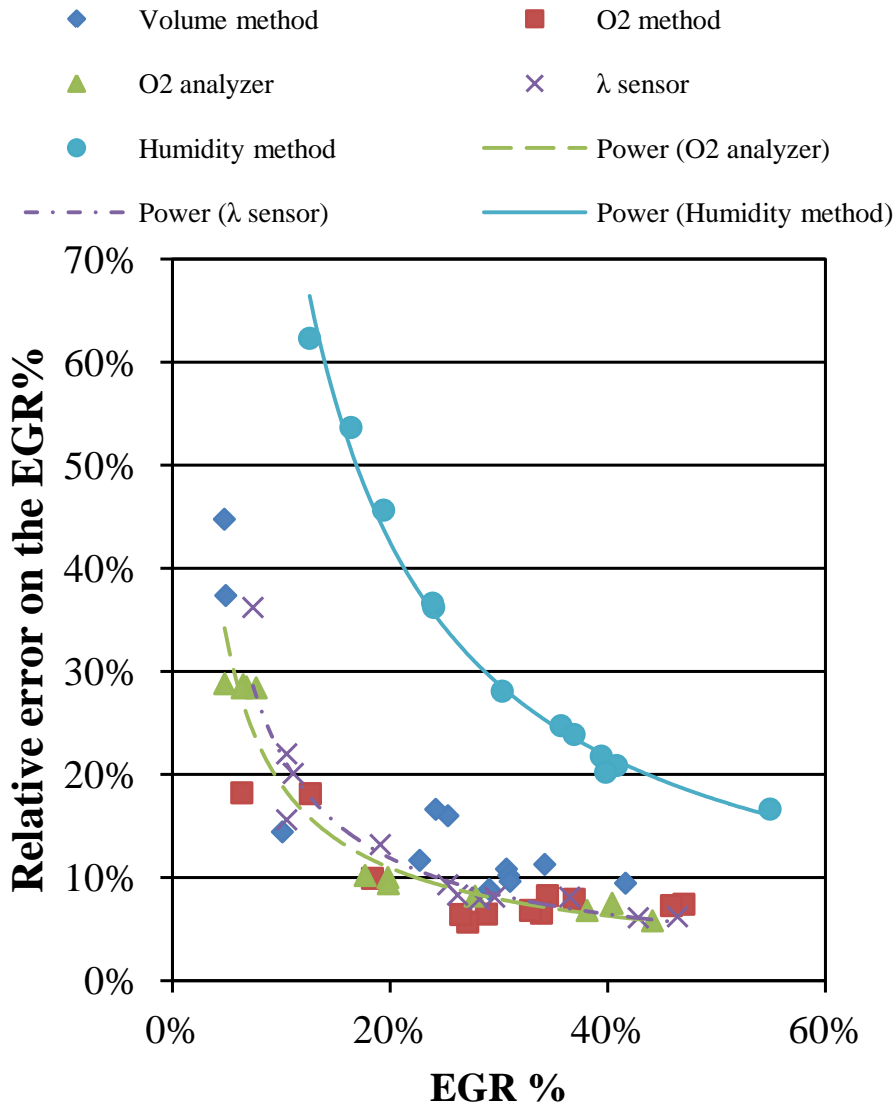


Figure 7: Comparison of the relative error on EGR% calculated using three different methods. Method 1 and 2 - dataset 1. Method 2(a), 2(b) and 3 - dataset 2. Error on the relative humidity $\delta\phi = 3.5\%$

The significant measurement errors for the first method are δQ_{air} and δQ_{H_2} and for the second method δy_{O_2} , δQ_{air} and δQ_{H_2} . With the values defined in Table 2, the relative error on the EGR% is calculated for all twelve samples of the first dataset and given as a function of the EGR% in Figure 6, where a trend

line is added. We see that all methods follow the same trend, a rising relative error for decreasing EGR%. Additionally, we see that the relative error for the second method is markedly smaller than that for the first method.

The errors for method 2(a) and 2(b), calculated based on dataset 2, and method 2, calculated based on dataset 1, are very similar. The relative errors for method 2 and dataset 1 are slightly lower, as the first dataset was obtained in stoichiometric conditions and the second dataset in lean conditions. As can be seen from Equation 26 lean conditions lead to larger values for c_1 , c_2 and c_3 and thus a larger relative error. Method 3 produces the largest errors. Even in the case of a carefully calibrated sensor ($\delta\phi=1.5\%$) the error is still higher than for the other methods.

6. Discussion

The relative error on the EGR%, obtained with the experiments in Figure 6, can be compared to the theoretically obtained relative error in Figure 4 for all methods. We observe that the error rises exponentially with decreasing EGR% for both figures. Considering the relative position of the error for the first two methods, the same conclusion can be drawn from theory and experimental data. Over the entire EGR%-range the second method is more accurate than the first method, especially for EGR% lower than 20%. The third method, however, leads to EGR% errors that are significantly larger than the theoretical curve in Figure 4. This is a results of the very small value for the error on the water vapor concentration ($\delta y_{H_2O}=0.005\%$) that was applied in the theoretical calculation. This would correspond to an error in the relative humidity of less than 0.5%, whereas a realistic lower limit for this error is 1.5%. Even with the minimal achievable error of 1.5%, the error associated with method 3 is well above that of the other two methods.

The trendlines in Figure 6 and lines in Figure 4 do not match completely. The experimental trendline of the relative error is shifted towards lower EGR% compared to the theoretically obtained line. This can be ascribed to the large variation in engine speed and λ in the dataset, which has a large influence on the EGR% (see Section 3). A better match could likely be obtained if each sample was taken at the same engine speed and volumetric efficiency.

If a proposed method is adopted, it is necessary to know which measurement device has the largest influence on the error. For each method, the equation of the relative error has only one measurement error with a coefficient depending on the EGR%. As can be seen in Figure 6 and 4 this measurement error will have the biggest influence for low amounts of EGR. The influence of the other measurement devices can be visualized by taking the EGR% limit of 100%, because then the measurement error depending on the EGR% has no influence on the error. These are very small for all three methods. In conclusion we can state that for the first method the accuracy of the air mass flow, for the second method of the O_2 -concentration and for the third method of the relative humidity measurement device are vital.

The discussion above only takes the influence of measurement errors into account. The calculated EGR% will also differ from the actual value due to assumptions made in the theoretical setup of the methods. The difference of EGR% between the first and second method in Figure 5 is a result of such an assumption.

For the first method the influence of the primary assumptions was investigated experimentally. In Section 2.2 a constant volumetric efficiency is presumed, irrespective of changes in intake temperature or gas properties. However, increasing the amount of exhaust gases in the intake charge, will rise its temperature and result in a reduced volumetric efficiency (defined based on the mass flow of fresh air and EGR into the cylinder). Tests were conducted on a direct-injection 500cc SI engine to investigate the influence of that assumption by measuring the air flow into the cylinder at various intake temperatures (Figure 8). It can be observed that there is a correlation between the intake temperature and the mass and volume flow of air into the engine cylinder. Through this correlation a scaling factor is derived and applied to the equation of the EGR% to neutralize the effect of varying temperature. This results in an increase in EGR% of approximately 2%.

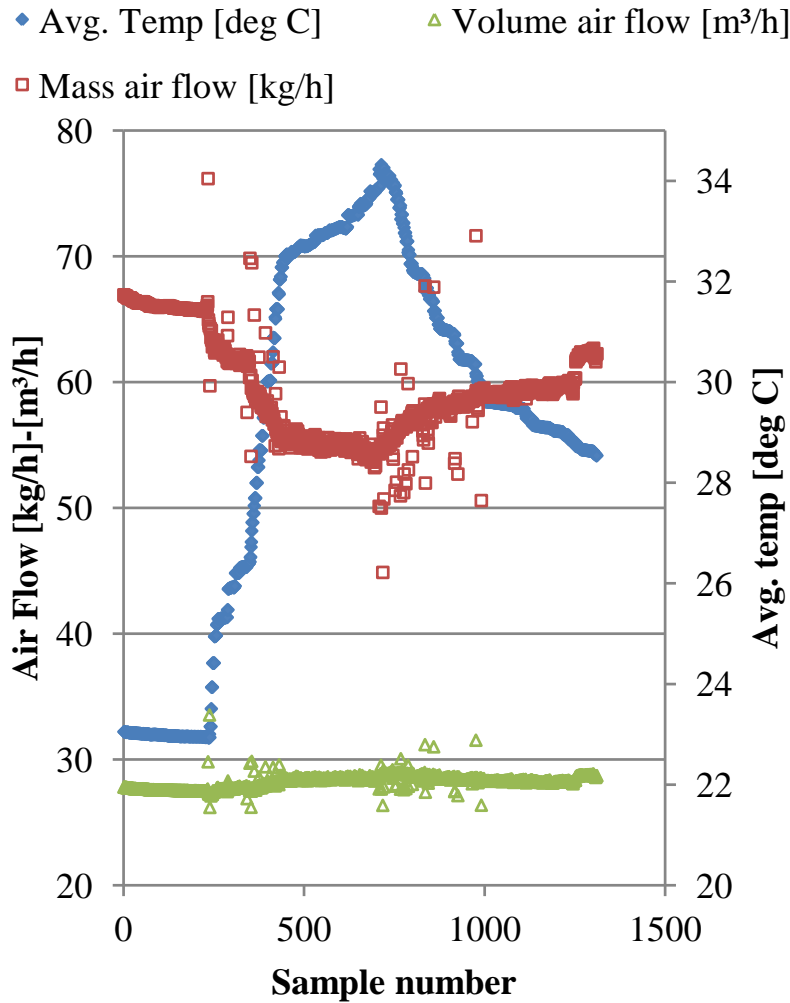


Figure 8: Investigation of the correlation between intake temperature and intake air volume on a direct-injection 500 cc single cylinder SI engine

In the experimental results of Section 5, however, this has only a minor influence due to the use of an EGR cooler. It reduces the exhaust gas temperature to 25°C, which is only slightly higher than the air temperature of 22°C.

The third method is based on a relative humidity measurement. Relative humidity sensors are calibrated in a climate chamber with a controlled humidity. However, exhaust gas has a different composition than the gas used for the calibration. This will affect the accuracy of the measurement depending on the exact gas composition and thus on different factors such as air-fuel ratio, engine load, EGR%, etc. Measuring the relative humidity in exhaust gas with a

conventional relative humidity sensor adds an additional source for error on the
calculated EGR% besides the measurement error, further limiting the practical
470 use of method 3.

Unlike the first and third method, for the second method, there are no
principal assumptions that could significantly influence the calculated EGR%
in the theoretical development of the equation of the EGR rate.

7. Conclusions

475 Three methods to determine the amount of EGR in a hydrogen ICE have
been developed and tested for their accuracy by means of an error analysis. The
first method is based upon a volume balance in the mixing section of exhaust
gases and fresh air. The second and third method use a molar balance of O_2
and H_2O respectively. Engine measurements were performed to validate the
480 theoretical analysis.

For all methods, the relative error on the calculated EGR% rises exponen-
tially with decreasing EGR%. Overall, the second method, based on a molar
balance of O_2 , results in the lowest relative errors. The third method seems
least practical, as the relative humidity sensors used in this method do not have
485 the required accuracy to ensure an acceptable error on the calculated EGR%.

In addition to the error analysis, the assumptions to develop the theoretical
equations and the feasibility of a method should be considered as well. The first
method is easy to implement in an engine, but assumes a constant volumetric
efficiency. This assumption was shown to be incorrect, as the change in inlet
490 temperature caused by the hot EGR gases can change the volumetric efficiency
and should be corrected for. The equation for the EGR rate of the second
method is developed without any assumptions. To apply this method only one
extra oxygen sensor is needed. This can be an O_2 gas analyzer, for stationary
applications, or a wide band lambda sensor, for production engines. The third
495 method needs relative humidity sensors, which are usually not present on an
engine. Furthermore, this method assumes that a humidity measurement can
be applied to exhaust gases, whereas such a sensor is generally calibrated in a
humidity chamber with moist air.

Taking into account the assumptions of each method, the error analysis
500 performed on the amount of EGR and the relative simplicity of implementation,
the method based on an oxygen molar balance is concluded to be the best
practice for determining the EGR rate in hydrogen engines.

Acknowledgements

J. Vancoillie acknowledges a Ph. D. fellowship (FWO09/ASP/030) of the
505 Research Foundation - Flanders (FWO). The Research Foundation - Flanders
has also funded the experimental equipment (1.5.147.10N). The authors would
like to thank Interreg IV for its support through the project HYDROGEN RE-
GION Flanders - South Netherlands.

Parts of the submitted manuscript have been created by UChicago Argonne,
510 LLC, Operator of Argonne National Laboratory ('Argonne'). Argonne, a U.S.
Department of Energy Office of Science laboratory, is operated under Contract
No. DE-AC02-06CH11357. The U.S. Government retains for itself, and others
acting on its behalf, a paid-up nonexclusive, irrevocable worldwide license in said
article to reproduce, prepare derivative works, distribute copies to the public,
515 and perform publicly and display publicly, by or on behalf of the Government.

Part of the research referenced in this manuscript was funded by DOE's
FreedomCAR and Vehicle Technologies Program, Office of Energy Efficiency
and Renewable Energy. T. Wallner wishes to thank Gurpreet Singh and Lee
Slezak, program managers at DOE, for their support. A hydrogen engine used
520 to run certain experiments presented in this manuscript was provided by Ford
Motor Company. Special thanks to the team from Ford Motor Company for
their support.

Bibliography

- 525 [1] Verhelst S, Wallner T. Hydrogen-fueled internal combustion engines. *Prog Energ Combust* 2009;35(6):490–527.
- [2] Abbott D. Keeping the energy debate clean: How do we supply the world’s energy needs? *Proc IEEE* 2010;98(1):42–66.
- [3] Das LM. Hydrogen engines: A view of the past and a look into the future. *Int J Hydrogen Energ* 1990;15(6):425–43.
- 530 [4] Matthias NS, Wallner T, Scarcelli R. A hydrogen direct injection engine concept that exceeds U.S. DOE light-duty efficiency targets. *SAE International*; 2012. SAE paper no. 2012-01-0653.
- [5] Verhelst S, Maesschalck P, Rombaut N, Sierens R. Increasing the power output of hydrogen internal combustion engines by means of supercharging and exhaust gas recirculation. *Int J Hydrogen Energ* 2009;34(10):4406–12.
- 535 [6] Wallner T, Nande AM, Scarcelli R. Evaluation of exhaust gas recirculation (EGR) in combination with direct injection (DI) on a hydrogen research engine. In: *3rd World Hydrogen Technology Convention*. Delhi, India; 2009, p. 1–6.
- 540 [7] Beck NJ, Wong HC, Gebert K. Clean air power inc., assignee. EGR control system and method for an internal combustion engine. United States Patent US 6,742,335; 2004 July 11.
- [8] Heffel JW. NOx emission reduction in a hydrogen fueled internal combustion engine at 3000 rpm using exhaust gas recirculation. *Int J Hydrogen Energ* 2003;28(11):1285–92.
- 545 [9] Szwaja S, Naber JD. Exhaust gas recirculation strategy in the hydrogen SI engine. In: *Journal of KONES 2007: Powertrain and Transport*; vol. 14. Warsaw, Poland; 2007, p. 1–8.
- [10] Verhelst S, Sierens R. Hydrogen engine-specific properties. *Int J Hydrogen Energ* 2001;26(9):987–90.
- 550 [11] Alduchov OA, Eskridge RE. Improved magnus form approximation of saturation vapor pressure. *J Appl Meteorol* 1996;35(4):601–9.
- [12] Taylor JR. *An introduction to Error Analysis*. Sausalito, CA: University Science Books; 2nd ed.; 1997.

555 **Appendix A. Accuracy calculation of the methods to determine the EGR rate**

Appendix A.1. General accuracy equation of the error made on the EGR%

We start from the definition of the EGR% (equation 1):

$$EGR\% = \frac{\dot{m}_{EGR}}{\dot{m}_{EGR} + \dot{m}_{air} + \dot{m}_{H_2}}$$

By applying Taylor, we obtain the error on the EGR% (squared):

$$\delta EGR\%^2 = \frac{(\dot{m}_{air} + \dot{m}_{H_2})^2 \cdot \delta \dot{m}_{EGR}^2 + \dot{m}_{EGR}^2 \cdot (\delta \dot{m}_{air}^2 + \delta \dot{m}_{H_2}^2)}{(\dot{m}_{EGR} + \dot{m}_{air} + \dot{m}_{H_2})^4}$$

560 Equation 19 shows that the error on the EGR% depends on three errors: $\delta \dot{m}_{EGR}$, $\delta \dot{m}_{air}$ and $\delta \dot{m}_{H_2}$. The parameters \dot{m}_{EGR} , \dot{m}_{air} and \dot{m}_{H_2} determine the weight of these errors.

To simplify this equation two assumptions are made:

- 565 1. \dot{m}_{H_2} is neglected with regard to \dot{m}_{air} . To justify this, we extract the ratio of \dot{m}_{H_2} and \dot{m}_{air} out of the equation for λ :

$$\lambda = \frac{L_w}{L_s} = \frac{1}{L_s} \cdot \frac{\dot{m}_{air}}{\dot{m}_{H_2}} \Rightarrow \frac{\dot{m}_{H_2}}{\dot{m}_{air}} = \frac{1}{34.2 \cdot \lambda} \quad (A.1)$$

with L_s the stoichiometric AFR for hydrogen combustion in air as 34.2:1. We conclude that the assumption can be made, as \dot{m}_{H_2} , for $\lambda=1$, only amounts to 3% of \dot{m}_{air} .

- 570 2. $\delta \dot{m}_{H_2}^2$ is neglected with regard to $\delta \dot{m}_{air}^2$. Applying Taylor on the ratio of \dot{m}_{H_2} and \dot{m}_{air} with $\dot{m}_{H_2} = \rho_{H_2} \cdot Q_{H_2}$ and $\dot{m}_{air} = \rho_{air} \cdot Q_{air}$ gives:

$$\frac{\delta \dot{m}_{H_2}^2}{\delta \dot{m}_{air}^2} = \frac{(\rho_{H_2} \cdot \delta Q_{H_2})^2}{(\rho_{air} \cdot \delta Q_{air})^2} = 0.005 \cdot \frac{\delta Q_{H_2}^2}{\delta Q_{air}^2} \quad (A.2)$$

This means that if the errors δQ_{H_2} and δQ_{air} have a similar dimension, equation A.2 justifies the second assumption. In case a device is utilized that measures \dot{m}_{air} and \dot{m}_{H_2} directly, this assumption is justified because normally the ratio of the errors $\delta \dot{m}_{H_2}$ and $\delta \dot{m}_{air}$ is similar to the ratio of equation A.1.

575

With these assumptions equation 19 is simplified to:

$$\delta EGR\%^2 = \frac{\dot{m}_{air}^2}{(\dot{m}_{EGR} + \dot{m}_{air})^4} \cdot \delta \dot{m}_{EGR}^2 + \frac{\dot{m}_{EGR}^2}{(\dot{m}_{EGR} + \dot{m}_{air})^4} \cdot \delta \dot{m}_{air}^2 \quad (A.3)$$

To further simplify this equation four substitutions can be made. When we neglect \dot{m}_{H_2} with regard to \dot{m}_{air} in equation 18, we can derive the first three equations to substitute:

$$\frac{\dot{m}_{EGR}^2}{(\dot{m}_{EGR} + \dot{m}_{air})^2} = EGR\%^2 \quad (A.4)$$

$$\frac{\dot{m}_{air}^2}{(\dot{m}_{EGR} + \dot{m}_{air})^2} = EGR\%^2 \cdot \frac{\dot{m}_{air}^2}{\dot{m}_{EGR}^2} \quad (A.5)$$

$$\dot{m}_{EGR} = \dot{m}_{air} \cdot \frac{EGR\%}{1 - EGR\%} \quad (A.6)$$

580 The fourth equation is found in the definition of the volumetric efficiency, which is defined as the ratio of the actual mass entering the cylinder to the theoretical mass capacity in the cylinder at a certain engine speed n :

$$\lambda_l = \frac{m_{actual}}{m_{theor}} = \frac{\dot{m}_{actual}}{m_{theor} \cdot n \cdot \chi} = \frac{\dot{m}_{EGR} + \dot{m}_{air} + \dot{m}_{H_2}}{m_{theor} \cdot n \cdot \chi} \quad (A.7)$$

with $\chi = \frac{1}{2}$ for four-stroke engines and m_{theor} depending on the actual air-fuel ratio (λ), the amount of EGR and the cylinder volume. Neglecting \dot{m}_{H_2} with regard to \dot{m}_{air} in this equation gives an expression for $(\dot{m}_{EGR} + \dot{m}_{air})$, which is the fourth and final substitution that has to be made.

At this point, equation 19 is reshaped to a general equation of the relative error on the EGR%:

$$\left(\frac{\delta EGR\%}{EGR\%}\right)^2 = \frac{1}{(\lambda_l \cdot m_{theor} \cdot n \cdot \chi)^2} \cdot \left(\frac{(1 - EGR\%)^2}{EGR\%^2} \cdot \delta \dot{m}_{EGR}^2 + \delta \dot{m}_{air}^2\right)$$

Appendix A.2. Accuracy equation of the error on the EGR% for method 1

590 In Section 2.2 we found that the EGR mass rate is equal to:

$$\dot{m}_{EGR} = \rho_{EGR} \cdot \Delta Q_{air}$$

Applying Taylor on this equation and combining equation A.6 with equation 21 to eliminate ΔQ_{air} gives:

$$\delta \dot{m}_{EGR}^2 = \rho_{EGR}^2 \cdot \delta \Delta Q_{air}^2 + \frac{EGR\%^2}{(1 - EGR\%)^2} \cdot \dot{m}_{air}^2 \cdot \frac{\delta \rho_{EGR}^2}{\rho_{EGR}^2} \quad (A.8)$$

We identify two errors:

1. $\delta \Delta Q_{air}$, calculated by applying Taylor on $\Delta Q_{air} = Q_{air,0} - Q_{air,1}$ and equal to $\sqrt{2} \cdot \delta Q_{air}$.

2. $\delta\rho_{EGR}$, the error on the density of the exhaust gases. This error is calculated by applying Taylor on equation 5. Neglecting the temperature and pressure errors we get:

$$\frac{\delta\rho_{EGR}}{\rho_{EGR}} = \frac{\delta R_{EGR}}{R_{EGR}} \quad (\text{A.9})$$

δR_{EGR} is calculated in Appendix B and depends on the errors $\delta\dot{m}_{air}$ and $\delta\dot{m}_{H_2}$; consequently, $\delta\rho_{EGR}$ too.

When using the first expression of equation B.6 for the error δR_{EGR} and by substituting equation A.8 in equation 20, we obtain an equation of the relative error on the EGR%:

$$\left(\frac{\delta\text{EGR}\%}{\text{EGR}\%}\right)^2 = \frac{1}{(\lambda_l \cdot m_{theor} \cdot n \cdot \chi)^2} \cdot (c_1 \cdot \delta\dot{m}_{air}^2 + c_2 \cdot \delta\dot{m}_{H_2}^2)$$

With:

$$c_1 = 2 \cdot \left(\frac{\rho_{EGR}}{\rho_{air}}\right)^2 \cdot \frac{(1 - \text{EGR}\%)^2}{\text{EGR}\%^2} + 1 + \frac{2698.77}{\left(1 + \frac{0.029}{\lambda}\right)^4} \cdot \frac{1}{R_{EGR}^2} \cdot \frac{1}{\lambda^2}$$

$$c_2 = \frac{2698.77 \cdot L_s^2}{\left(1 + \frac{0.029}{\lambda}\right)^4} \cdot \frac{1}{R_{EGR}^2}$$

605 Appendix A.3. Accuracy equation of the error on the EGR% for method 2

The approach to find the influences on the error of the EGR% for method 2 is similar to section Appendix A.2: the error $\delta\dot{m}_{EGR}^2$ is calculated in this section and afterwards substituted in the general equation of the relative error on the EGR% (equation 20).

610 In section 2.3 we determined the EGR mass rate as:

$$\dot{m}_{EGR} = \frac{1}{MW_{air}} \cdot \dot{m}_{air} \cdot MW_{EGR} \cdot \Delta y_{O_2}$$

Applying Taylor gives:

$$\delta\dot{m}_{EGR}^2 = \left(\frac{MW_{EGR}}{MW_{air}}\right)^2 \cdot \left(\Delta y_{O_2}^2 \cdot \delta\dot{m}_{air}^2 + \dot{m}_{air}^2 \cdot \delta\Delta y_{O_2}^2 + \dot{m}_{air}^2 \cdot \Delta y_{O_2}^2 \cdot \frac{\delta MW_{EGR}^2}{MW_{EGR}^2}\right) \quad (\text{A.10})$$

We identify three errors:

1. $\delta\dot{m}_{air}$, defined by the measuring device;

- 615 2. $\delta\Delta y_{O_2}$, calculated by applying Taylor on $\Delta y_{O_2} = \frac{y_{O_2,air} - y_{O_2,mix}}{y_{O_2,mix} - y_{O_2,EGR}}$. This calculation is written out in Appendix C;
3. δMW_{EGR} , calculated in Appendix B and depending on the errors $\delta\dot{m}_{air}$ and $\delta\dot{m}_{H_2}$.

To eliminate Δy_{O_2} in equation A.10 we combine equation A.6 with equation 12. Using the first expression of equation B.5 for δMW_{EGR} , we obtain that the
620 relative error on the EGR% is equal to:

$$\left(\frac{\delta EGR\%}{EGR\%}\right)^2 = \frac{1}{(\lambda_l \cdot m_{theor} \cdot n \cdot \chi)^2} \cdot (c_1 \cdot \delta\dot{m}_{air}^2 + c_2 \cdot \delta\dot{m}_{H_2}^2 + c_3 \cdot \delta y_{O_2}^2)$$

with:

$$\begin{aligned} c_1 &= \frac{2.7 \cdot 10^{-5}}{\left(1 + \frac{0.21}{\lambda}\right)^4} \cdot \frac{1}{MW_{EGR}^2} \cdot \frac{1}{\lambda^2} + 2 \\ c_2 &= \frac{2.7 \cdot 10^{-5}}{\left(1 + \frac{0.21}{\lambda}\right)^4} \cdot \frac{L_s^2}{MW_{EGR}^2} \\ c_3 &= \frac{\dot{m}_{air}^2}{(y_{O_2,mix} - y_{O_2,EGR})^2} \cdot \left(2 + \frac{2}{x} \cdot \frac{(1 - EGR\%)}{EGR\%} + \frac{1}{x^2} \cdot \frac{(1 - EGR\%)^2}{EGR\%^2}\right) \end{aligned}$$

and $x = \frac{MW_{air}}{MW_{EGR}}$.

Appendix A.4. Accuracy equation of the error on the EGR% for method 3

In Section 2.4 we determined the EGR mass rate as:

$$\dot{m}_{EGR} = \frac{1}{MW_{air}} \cdot \dot{m}_{air} \cdot MW_{EGR} \cdot \Delta y_{H_2O}$$

625 which is similar to \dot{m}_{EGR} of method 2. Consequently, applying Taylor results in similar equation as in Section Appendix A.3:

$$\delta\dot{m}_{EGR}^2 = \left(\frac{MW_{EGR}}{MW_{air}}\right)^2 \cdot \left(\Delta y_{H_2O}^2 \cdot \delta\dot{m}_{air}^2 + \dot{m}_{air}^2 \cdot \delta\Delta y_{H_2O}^2 + \dot{m}_{air}^2 \cdot \Delta y_{H_2O}^2 \cdot \frac{\delta MW_{EGR}^2}{MW_{EGR}^2}\right) \quad (A.11)$$

Three errors are identified: $\delta\dot{m}_{air}$ and δMW_{EGR} which are defined as in Section Appendix A.3; and Δy_{H_2O} , which is calculated by applying Taylor on:

$$\Delta y_{H_2O} = \frac{y_{H_2O,air} - y_{H_2O,mix}}{y_{H_2O,mix} - y_{H_2O,EGR}} \quad (A.12)$$

Differently from Section 3.3, $\delta\Delta y_{H_2O}$ depends on δy_{H_2O} which is at its turn
630 calculated by applying Taylor on:

$$y_{H_2O} = \frac{\phi \cdot p_s}{p} \quad (\text{A.13})$$

and consequently depends on the pressure, saturation pressure and relative humidity at the places according to Figure 1. The calculations to obtain an equation for $\delta\Delta y_{H_2O}$ are described in Appendix C.

To eliminate Δy_{H_2O} in equation A.11, we combine equation A.6 with equation 12. With all these substitutions we obtain a similar equation as in Section 3.3 for the relative error on the EGR%, but with the error δO_2 replaced by $\delta y_{H_2O,av}$ (as in Equation C.7) and a different coefficient c_3 :

$$\left(\frac{\delta EGR\%}{EGR\%}\right)^2 = \frac{1}{(\lambda_l \cdot m_{theor} \cdot n \cdot \chi)^2} \cdot (c_1 \cdot \delta \dot{m}_{air}^2 + c_2 \cdot \delta \dot{m}_{H_2}^2 + c_3 \cdot \delta y_{H_2O,av}^2)$$

with:

$$\begin{aligned} c_1 &= 2 + \frac{2.7 \cdot 10^{-5}}{\left(1 + \frac{0.21}{\lambda}\right)^4} \cdot \frac{1}{\lambda^2} \cdot \frac{1}{MW_{EGR}^2} \\ c_2 &= \frac{2.7 \cdot 10^{-5}}{\left(1 + \frac{0.21}{\lambda}\right)^4} \cdot \frac{L_s^2}{MW_{EGR}^2} \\ c_3 &= \frac{\dot{m}_{air}^2}{(y_{H_2O,mix} - y_{H_2O,EGR})^2} \cdot \left(2 + \frac{2}{x} \cdot \frac{(1 - EGR\%)}{EGR\%} + \frac{2}{x^2} \cdot \frac{(1 - EGR\%)^2}{EGR\%^2}\right) \end{aligned}$$

and $x = \frac{MW_{air}}{MW_{EGR}}$.

640 Appendix B. Calculation of R_{EGR} and MW_{EGR} and their accuracy

The specific gas constant and molar weight of the re-circulated exhaust gases, are determined by the combustion reaction of hydrogen. As can be seen in equation 2 the main combustion products are H_2O , N_2 and respectively O_2 or H_2 for $\lambda \geq 1$ or $\lambda < 1$. The molar weight of the exhaust gas is a function of the molar weights of its components:

$$MW_{EGR} = \begin{cases} \lambda \geq 1 : y_{H_2O} \cdot MW_{H_2O} + y_{N_2} \cdot MW_{N_2} + y_{O_2} \cdot MW_{O_2} \\ \lambda < 1 : y_{H_2O} \cdot MW_{H_2O} + y_{N_2} \cdot MW_{N_2} + y_{H_2} \cdot MW_{H_2} \end{cases} \quad (\text{B.1})$$

with y the mole fraction of the subscripted gas, calculated out of the combustion reaction. The specific gas constant is calculated analogously, except according to the units of R , mass fractions instead of mole fractions are used:

$$R_{EGR} = \begin{cases} \lambda \geq 1 : c_{H_2O} \cdot R_{H_2O} + c_{N_2} \cdot R_{N_2} + c_{O_2} \cdot R_{O_2} \\ \lambda < 1 : c_{H_2O} \cdot R_{H_2O} + c_{N_2} \cdot R_{N_2} + c_{H_2} \cdot R_{H_2} \end{cases} \quad (\text{B.2})$$

650 Calculating the molar weight and the specific gas constant of the exhaust gases defined as above gives:

$$MW_{EGR} = \begin{cases} \lambda \geq 1 : \frac{5.12 \cdot \lambda + 0.15}{177.41 \cdot \lambda + 37.12} \\ \lambda < 1 : \frac{0.26 \cdot \lambda + 0.21}{12.53 \cdot \lambda + 6.63} \end{cases} \quad (\text{B.3})$$

$$R_{EGR} = \begin{cases} \lambda \geq 1 : \frac{1774.15 \cdot \lambda + 371.16}{6.15 \cdot \lambda + 0.18} \\ \lambda < 1 : \frac{14029.87 \cdot \lambda + 7423.21}{34.75 \cdot \lambda + 28.57} \end{cases} \quad (\text{B.4})$$

With λ defined by equation A.1 and applying equation 17 on MW_{EGR} and R_{EGR} , we obtain the absolute errors on MW_{EGR} and R_{EGR} , squared:

$$\delta MW_{EGR}^2 = \begin{cases} \lambda \geq 1 : \frac{2.7 \cdot 10^{-5} \cdot L_s^2}{\left(1 + \frac{0.21}{\lambda}\right)^4} \cdot \frac{1}{\dot{m}_{air}^2} \cdot \left(\frac{1}{(\lambda \cdot L_s)^2} \cdot \delta \dot{m}_{air}^2 + \delta \dot{m}_{H_2}^2 \right) \\ \lambda < 1 : \frac{3.63 \cdot 10^{-5} \cdot L_s^2}{\left(1 + \frac{0.53}{\lambda}\right)^4} \cdot \frac{1}{\dot{m}_{air}^2} \cdot \left(\frac{1}{(\lambda \cdot L_s)^2} \cdot \delta \dot{m}_{air}^2 + \delta \dot{m}_{H_2}^2 \right) \end{cases} \quad (\text{B.5})$$

$$\delta R_{EGR}^2 = \begin{cases} \lambda \geq 1 : \frac{2698.77 \cdot L_s^2}{\left(1 + \frac{0.029}{\lambda}\right)^4} \cdot \frac{1}{\dot{m}_{air}^2} \cdot \left(\frac{1}{(\lambda \cdot L_s)^2} \cdot \delta \dot{m}_{air}^2 + \delta \dot{m}_{H_2}^2 \right) \\ \lambda < 1 : \frac{14003.16 \cdot L_s^2}{\left(1 + \frac{0.822}{\lambda}\right)^4} \cdot \frac{1}{\dot{m}_{air}^2} \cdot \left(\frac{1}{(\lambda \cdot L_s)^2} \cdot \delta \dot{m}_{air}^2 + \delta \dot{m}_{H_2}^2 \right) \end{cases} \quad (\text{B.6})$$

655 Appendix C. Calculating the absolute error on Δy_{O_2} and Δy_{H_2O}

This first part of this appendix section will deal with the simplification of the error on Δy_{O_2} which is defined as:

$$\Delta y_{O_2} = \frac{O_{2,air} - O_{2,mix}}{O_{2,mix} - O_{2,EGR}} \quad (\text{C.1})$$

Applying Taylor on C.1 gives the error on Δy_{O_2} :

$$\delta \Delta y_{O_2}^2 = \frac{1}{(O_{2,mix} - O_{2,EGR})^2} \cdot ((\Delta y_{O_2} + 1)^2 + \Delta y_{O_2}^2) \cdot \delta O_2^2 \quad (\text{C.2})$$

660 with δO_2 the error of the oxygen measuring device. Combining equation A.6 with equation 12 gives an expression for Δy_{O_2} as a function of the EGR%:

$$\Delta y_{O_2} = \frac{MW_{air}}{MW_{EGR}} \cdot \frac{EGR\%}{1 - EGR\%} = x \cdot \frac{EGR\%}{1 - EGR\%} \quad (\text{C.3})$$

with $x = \frac{MW_{air}}{MW_{EGR}}$. Substituting equation C.3 in equation C.2 gives the expression for the absolute error on Δy_{O_2} :

$$\delta \Delta y_{O_2}^2 = 2 \cdot \left(x^2 \cdot \frac{(EGR\%)^2}{(1 - EGR\%)^2} + x \cdot \frac{EGR\%}{(1 - EGR\%)^2} + \frac{1}{2} \right) \cdot \frac{\delta O_2^2}{(O_{2,mix} - O_{2,EGR})^2} \quad (\text{C.4})$$

The second part of this appendix section deals with the simplification of the error on Δy_{H_2O} , which is calculated analogously as $\delta\Delta y_{O_2}$:

$$\delta\Delta y_{H_2O}^2 = \frac{(\delta y_{H_2O,air}^2 + \Delta y_{H_2O}^2 \cdot \delta y_{H_2O,EGR}^2 + (\Delta y_{H_2O} + 1)^2 \cdot \delta y_{H_2O,mix}^2)}{(y_{H_2O,mix} - y_{H_2O,EGR})^2} \quad (C.5)$$

665 However, the difference between equation C.2 and C.5 is that δy_{H_2O} depends on the pressure, saturation pressure, relative humidity and their errors through equation A.13:

$$\delta y_{H_2O}^2 = \frac{1}{p^2} \cdot \left(p_s^2 \cdot \delta\phi^2 + \phi^2 \cdot \delta p_s^2 + \left(\frac{\phi \cdot p_s}{p} \right)^2 \cdot \delta p^2 \right)^2 \quad (C.6)$$

If we define $\delta y_{H_2O,av}^2$, the average error on the mole fractions of H_2O , as:

$$\delta y_{H_2O,av}^2 = \frac{1}{3} \cdot (\delta y_{H_2O,air}^2 + \delta y_{H_2O,EGR}^2 + \delta y_{H_2O,mix}^2) \quad (C.7)$$

we can write equation C.5 similar to equation C.4:

$$\delta\Delta y_{H_2O}^2 = 2 \cdot \left(x^2 \frac{(EGR\%)^2}{(1 - EGR\%)^2} + x \frac{EGR\%}{(1 - EGR\%)} + 1 \right) \cdot \frac{\delta y_{H_2O,av}^2}{(y_{H_2O,mix} - y_{H_2O,EGR})^2} \quad (C.8)$$

670 Appendix D. Determination of the offset between method 1 and method 2 in Figure 5

The reason for the offset in Figure 5 can be explained by taken the ratio of the EGR rate of method 1 (equation 3):

$$\dot{m}_{EGR,method\ 1} = \rho_{EGR} \cdot \Delta Q_{air} \quad (D.1)$$

and the EGR rate of the second method (equation 12):

$$\dot{m}_{EGR,method\ 2} = \frac{1}{MW_{air}} \cdot \dot{m}_{air} \cdot MW_{EGR} \cdot \Delta y_{O_2} \quad (D.2)$$

675 Therefore equation D.1 is written as:

$$\dot{m}_{EGR,method1} = \frac{\rho_{EGR}}{\rho_{air}} \cdot \dot{m}_{air,1} \cdot \left(\frac{\dot{m}_{air,0}}{\dot{m}_{air,1}} - 1 \right) \quad (D.3)$$

with $\dot{m}_{air,0}$ and $\dot{m}_{air,1}$ respectively the EGR mass rate without use of EGR and with use of EGR. We obtain for the ratio:

$$\frac{\dot{m}_{EGR,method\ 1}}{\dot{m}_{EGR,method\ 2}} = \left(\frac{\dot{m}_{air,0}}{\dot{m}_{air,1}} - 1 \right) \cdot \frac{1}{\Delta y_{O_2}} \cdot \left(\frac{\rho_{EGR} \cdot MW_{air}}{\rho_{air} \cdot MW_{EGR}} \right) \quad (D.4)$$

We see from equation D.4 that the offset between the EGR rate (and by consequence the EGR% too) of method 1 and 2 depends on the variables of each method. Consequently, there will always be an offset, unless the variables are 680 neutralized by each other.

Appendix E. Experimental conditions

no.	speed [rpm]	λ	p_{gauge} [bar]	ignition [° ca BTDC]	torque [Nm]	BMEP [bar]	EGR% method 1	EGR% method 2
1	1800	0.97	0.0	-4	13.8	4.26	41.6%	47.0%
2	1800	0.97	0.0	-4	15.2	4.69	34.2%	45.8%
3	2250	1.00	0.0	-7	16.0	4.94	30.7%	36.9%
4	3000	1.00	0.0	-7	14.9	4.60	30.9%	34.5%
5	2750	0.99	0.0	-7	13.1	4.04	31.0%	33.9%
6	2000	0.99	0.0	-6	16.3	5.03	29.1%	32.9%
7	2000	0.98	0.0	-6	16.7	5.15	25.3%	28.9%
8	1800	0.97	0.5	-5	31.6	9.75	24.2%	27.1%
9	3000	0.97	0.7	-9	38.8	11.97	22.7%	26.5%
10	2250	0.97	0.5	-5	34.8	10.74	10.1%	18.4%
11	3000	0.97	0.5	-7	34.8	10.74	4.8%	12.7%
12	2250	0.97	0.7	-9	39.9	12.31	4.9%	6.4%
no.	speed [rpm]	λ	p_{gauge} [bar]	ignition [° ca BTDC]	torque [Nm]	BMEP [bar]	EGR% method 2(a)	EGR% method 2(b)
14	2000	1.01	0.0	-4	12.9	3.98	44.1%	42.8%
15	2000	1.29	0.0	-4	8.3	2.56	40.4%	36.5%
16	1500	1.05	0.0	-6	13.3	4.10	38.1%	46.4%
17	1500	1.00	0.0	-6	16.9	5.21	27.8%	29.6%
18	2000	1.31	0.0	-4	13.6	4.20	19.8%	26.2%
19	1500	1.02	0.0	-6	18.2	5.62	19.8%	25.3%
20	1500	1.25	0.0	-6	13.7	4.23	17.7%	28.2%
21	2000	1.70	0.0	-4	10.4	3.21	7.7%	7.4%
22	2000	1.60	0.0	-4	13.5	4.17	6.8%	19.1%
23	1500	1.19	0.0	-6	17.8	5.49	6.5%	10.5%
24	2000	1.92	0.0	-4	10.8	3.33	6.4%	11.1%
25	1500	1.61	0.0	-6	13.9	4.29	4.8%	10.5%

Table E.3: Experimental conditions